ELSEVIER

International Journal of Mass Spectrometry 202 (2000) 217–229

International Journal of Mass Spectrometry

Ion detection efficiency in SIMS: dependencies on energy, mass and composition for microchannel plates used in mass spectrometry

I.S. Gilmore*, M.P. Seah

Centre for Materials Measurement and Technology, National Physical Laboratory Queens Road, Teddington, Middlesex TW11 0LW, UK

Received 16 March 2000; accepted 24 April 2000

ABSTRACT

The effects of ion energy, mass and composition on the detection efficiency of a microchannel plate (MCP) have been studied in detail, using a time-of-flight (TOF) mass spectrometer. This spectrometer is used for static secondary ion mass spectrometry (static SIMS) although the data are relevant to any ion-detection system. A model is developed that shows how the efficiency falls with increased mass and decreased ion impact energy at the front of the MCP. At an impact energy of 20 keV, the efficiency for the detection of cationised PS oligomers of mass 10,000 amu is approximately 80%, whereas at 5 keV it has fallen to ~5%. The model is extended to estimate the effect of ion composition on the detection efficiency. It was found that ions with a high hydrogen content have a lower efficiency than those that consist of a cluster of high atomic number atoms. The spread of detection efficiencies arising from both composition and mass may be reduced by increasing the ion impact energy. Therefore, up to a mass of 4000 amu, the spread for ions of 100% observed for 5-keV ion impact energy is reduced to a negligible spread for ions of 20-keV impact energy, where the efficiency is approximately unity, independent of the composition. A simple method is provided to determine the correct voltage to operate the MCP for a given efficiency. This operating voltage should be determined for the highest mass ions in the required range. (Int J Mass Spectrom 202 (2000) 217–229) Crown copyright © 2000. Published by Elsevier Science B.V.

Keywords: Microchannel plate; Detector efficiency; Ion detection; Time-of-flight mass spectrometry; Static secondary ion mass spectrometry

1. Introduction

Microchannel plate detectors (MCPs) [1] are used widely for ion detection in time-of-flight (TOF) mass spectrometry. MCPs are compact, flat and have sub-nanosecond response times, making them ideal for time-of-flight applications. Channel electron multipliers (CEMs), which have been used for many years for both electron and ion detection, are not suitable for these systems. CEMs have conical entrance horns, which, for ions of the same mass, would lead to a spread in arrival times across the detector, leading to a loss in mass resolution in a TOF analyser. However, the importance of the CEM in techniques such as Auger electron spectroscopy (AES) and X-ray electron spectroscopy (XPS) has led to a detailed understanding of the electron detection efficiency of CEMs [2–6] and hence of their optimal use in practice. Essentially, an MCP is an array of continuous chan-

*Corresponding author. E-mail: Ian.Gilmore@npl.co.uk

PII S1387-3806(00)00245-1

nels, similar to those used in a CEM, but straight, so that much of the theoretical understanding for the CEM can be simply transferred. A recent study of the ion detection efficiency using CEMs [7,8] has shown that the established theories for electron detection are applicable, but with the first event replaced by the emission of electrons generated by the incident ions.

In mass spectrometry, the general relationship between the measured intensity, *I(c, m, E)*, and the true spectral intensity, *n(c, m, E)*, for a cluster, *c*, at a mass, *m*, and with energy, *E*, of those secondary ions that survive to the detector, is given approximately by

$$I(c,m,E,E_D) = T(m,E)\,D(c,m,E_D)\,F(m,E)n(c,m,E) \qquad (1)$$

In this equation, *T(m,E)* is the spectrometer transmission efficiency, $D(c, m, E_D)$ is the detector efficiency for ions impacting at energy E_D and *F(m, E)* is the transfer characteristic of the electronic counting system. In Eq. (1) we ignore any fragments arising from the decay of metastable ions. In the present work we study the term $D(c, m, E_D)$ for ions of masses up to 10,000 amu, for impact energies at the detector, E_D, between 0 and 20 keV and for clusters with a range of compositions.

The variation of $D(c,m,E_D)$ from one spectrometer to another, and also for one spectrometer over time, is a significant contribution to the poor reproducibility of spectra in static SIMS. In the past these effects have been overshadowed by poor instrument repeatability, but now many instruments can achieve an excellent repeatability of 2% [9] or better. A knowledge of the behaviour of the term $D(c, m, E_D)$ is required to establish procedures that reduce the variations as much as possible. For some quantitative work, such as concentration measurement, spectral intensities need to be corrected using $D(c, m, E_D)$. Early studies by Rudat and Morisson [10] showed how the detection efficiency varied with atomic mass for single ions. They observed a periodic behaviour with broad maxima corresponding to F, K, Rb and Ba and minima at Mg, Ga, Cd and Pt, superimposed on a gradual decline in efficiency with mass, *m*, approximately as $m^{-0.1}$. The importance of mass spectrometry for elemental analysis has led to a detailed characterisation of detectors, particularly the discrete dynode types. However, these measurements are time consuming, and so schemes are used to predict the behaviour from a restricted measurement set [11]. It would be much simpler for analysts if the detector gave unity efficiency, with no variations, in their required mass range.

The advent of TOF mass analysers for SIMS, which are able to access a mass range up to 10,000 amu, has required an improved knowledge of the detection efficiency for large polyatomic ions. The detection efficiency of these heavy ions is low and sensitive to the precise operating conditions. Niehuis [12] used the electron yield measured for chromium clusters to estimate the effect of mass on detection efficiency for different values of the postacceleration energy, E_D. This shows the efficiency falling away with mass. Hagenhoff et al. [13] have used these curves to correct static SIMS spectra to improve the accuracy in the calculation of molecular weight distributions of PDMS oligomers. However, the detection efficiency is largely ignored in other static SIMS analyses.

Matrix assisted laser desorption ionisation (MALDI) has further increased the accessible mass range, providing ions with masses of 300,000 amu or more. The number of secondary electrons emitted by the detector surface at the initial impact is so low that the design of the detection system is critical. This has led to a number of studies of electron emission generated by large biological ions such as trypsin and albumin [14]. More recently, the interest in polyatomic primary ions for use in SIMS, and understanding the processes of ion emission, has led to more detailed studies of their secondary electron yields [20].

The ion-induced electron emission yield is composed of two processes, potential and kinetic emission [21]. Potential emission occurs if the ionisation potential of the impact ion is greater than double the work function of the target. Following neutralisation of the incoming ion, the excess energy liberates electrons via resonant Auger processes, providing a small constant yield as a function of energy [22]. Kinetic emission is caused directly by the interaction

of the primary ion with target atoms as it moves through the material. A number of theories have been developed to account for the complex functionality of the emission yield. Some of these are reviewed elsewhere [21]. One of the first models was that developed by Parilis and Kishinevski [23]. Here, the generation of secondary electrons is described by a complex mechanism involving the cross section for electron-hole pair creation in the valence or conduction bands, followed by an Auger recombination process. The cross section used has an implicit energy threshold for emission that is equivalent to an ion impact velocity, v, of approximately 6×10^4 m/s, dependent on the ion and target. The emission yield, γ, is calculated by integration over the attenuating electron path to the surface. A term is introduced called the "straight line threshold" velocity, v_0, which gives the intersection, on the velocity axis, of the extrapolated linear part of the γ dependence on v. This model predicts the functionality of the secondary electron emission yield, γ, to have three regions:

1. $\gamma \propto v^4$ for velocities below v_0;
2. $\gamma \propto v^2$ for velocities at around v_0;
3. $\gamma \propto v$ for velocities above v_0.

This model has been shown to fit the data of Arifov and Rakhimov [24] for singly charged argon ions impacting a molybdenum target with velocities between 0.6×10^5 m/s to 1.2×10^5 m/s. However, Beuhler and Friedman [25] have found that this model does not fit well, with reasonable values of the parameters, for their work studying high molecular weight ions.

Beuhler and Friedman [25] have extended the concepts of Sternglass [26] for energies above 100 keV. In that model, the energy available for ionisation is proportional to the rate of energy loss, i.e., the sum of the nuclear and electronic stopping powers. Similarly to the theory of Parilis and Kishinevski, the emission yield is calculated by integration with the electron attenuation over the range of the ion. The nuclear stopping power they use is independent of the ion energy but the electron stopping power is proportional to ion velocity. At low velocity, where the range of the ion is within the secondary electron escape depth, the electron emission rises with a high power dependence on velocity. At high energies, the theory reduces to that of Sternglass, with the yield proportional to velocity. There is no velocity threshold in this model below which no emission occurs. This is in agreement with recent sensitive experiments with large biomolecules at velocities below 1×10^4 m/s. This model provide a good fit with data for H_2O clusters [27,28] extending up to masses of 50,000 amu. They found that the electron emission yield produced by polyatomic ions on a copper target is simply the sum of the yields from the constituent atoms [27]. Additivity was found to be obeyed for clusters with velocities below 1×10^5 m/s. However, for an insulating target Al_2O_3, the yield was less than the summed yield. For a given impact velocity, an empirical relationship between the electron emission yield and mass has shown the electron emission yield to exhibit a power dependence on the ion mass. The index of this power has been found in a number of studies [16,18,20] to be approximately 0.7.

2. Experimental

The instrument used in this study, an ION-TOF (Münster) SIMS IV, is of an open structure, single-stage reflectron design [29]. The instrument is equipped with a high resolution Ga^+ focused liquid metal ion gun with an energy range between 12 and 25 keV, mounted at 45° to the sample surface normal. The equipment is described in more detail elsewhere [30]. In the present study 15-keV gallium primary ions were digitally rastered with a 128×128 array over an area of 200 μm $\times$ 200 μm on the surface using a pulsed beam current of 0.5 pA. The time between each primary ion pulse was set to 300 μs, giving a mass range up to 3900 amu. Each spectrum was acquired for 60 s, giving a total ion surface dose of 5×10^{15} ions/m^2. To ensure the ion dose was uniform over the entire raster area, the spot size was defocused to be greater than 3 μm. Spectra were acquired from a fresh area of a square array for each condition. The centre-to-centre separation of the array

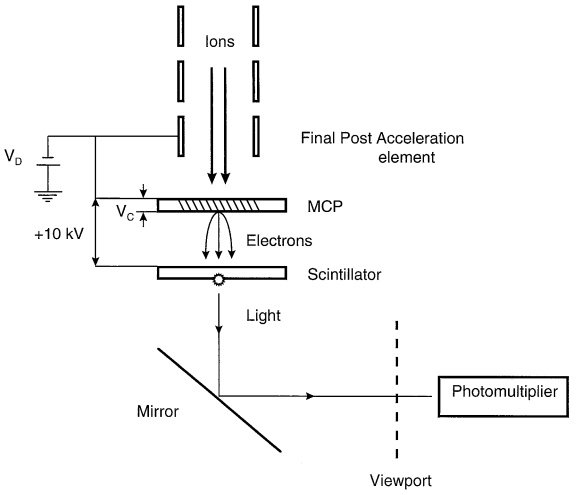

Fig. 1. Schematic of the ion detection system used in this TOF SIMS spectrometer.

was 700 μm and all of the analysis areas were at least 2.5 mm from the edge of the holder aperture.

The material analysed in this study is a thin polystyrene (PS) film, with a molecular weight of 2500, deposited on etched silver. Samples were prepared from a 1 mg/ml toluene solution using the procedure developed for the preparation of Irganox 1010 used in an interlaboratory study [9]. This method provided an evenly coated substrate that gave a good repeatability from area to area.

The ion detector arrangement for this system is shown in Fig 1. A single MCP is located after the last post-acceleration electrode. The surface is electrically connected to the final post-acceleration electrode at a voltage, V_D, which defines the impact energy, E_D. The voltage across the channel plate, V_C, is variable from 0 V to 1000 V. Following amplification by the cascades in the microchannels, the emitted plume of electrons is accelerated by nearly 10 kV to a scintillator with a thin surface film of aluminium. The resulting flashes of light mirror to a photomultiplier situated externally to the vacuum system. The advantage of using a method involving light is that it decouples the sensitive counting electronics from the high voltages present in the detector. This allows the use of accelerating voltages, for both positive and negative ions, to generate impact energies between 0 and 20 keV. This system can give shorter dead times than those that capacitively decouple the high voltage.

The MCP used in this study, supplied by Galileo, has an active area with a diameter of 18 mm, a channel size of 10 μm, a channel centre to channel centre spacing of 12 μm and a channel length to diameter ratio of 40:1. Each channel is inclined at an angle of 5° to the surface normal to maximise the electron yield for the incoming particle. The detection efficiency is limited to the fractional area presented by the channel, known as the open area ratio. For this MCP the open area ratio is determined as 54.5%. In the rest of this work the efficiencies analysed only relate to this open area.

3. Results

3.1. Effect of detector voltage

For an electron amplification cascade to develop along a microchannel, enough energy must be gained by emitted secondary electrons, so that the yield in the next event is sufficiently high to maintain the cascade. The gain [1,2], G, of an MCP with a secondary electron yield, δ is simply given by

$$G = \delta_1 \delta^p \quad (2)$$

where δ_1 is the ion-induced electron yield of the first event followed by p electron induced events. Of course, p is not a unique value for each event but is a statistical average. The secondary electron yield from the channel surface, δ, maximises at an energy above 400 eV. This energy is provided by a potential difference V_C applied across the front and rear faces of the MCP. The semiconducting surface of the channel acts as a continuous dynode with the potential becoming more positive toward the end of the channel. For this MCP, the applied voltage V_C is ~1000 V. The exact value of V_C will depend on the aspect ratio of the channels and so varies from one design to another. If p is approximately 10, δ is in a range where, approximately $\delta \propto V_C$, because the electron energies only reach some 100 eV for each impact in the amplification down a channel. As the applied

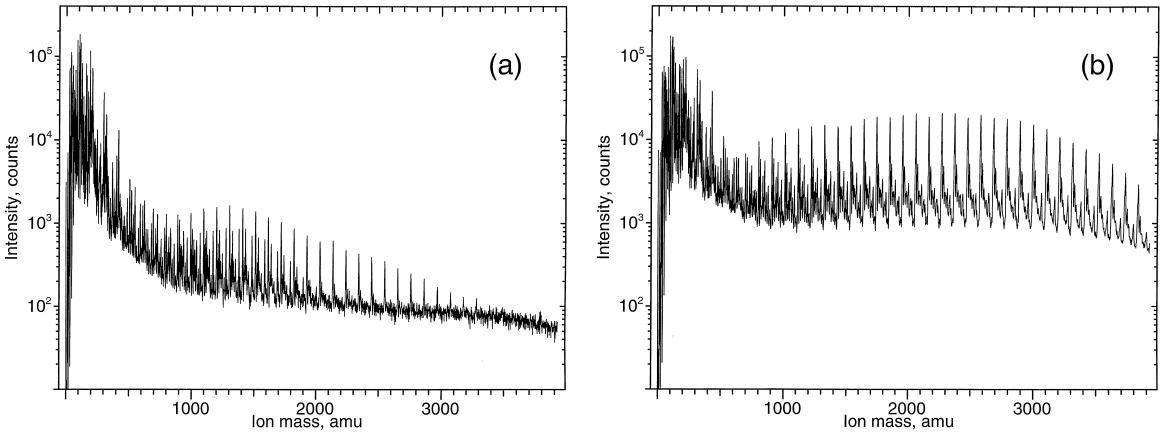

Fig. 2. Positive ion SIMS spectra of Ag cationised PS oligomers at 20 kV post-acceleration voltage with detector voltages, V_C, of (a) 650 V and (b) 950 V.

voltage is increased further the gain rises to a plateau, probably due to depletion of the channel wall current at the output end of the device.

The positive ion SIMS spectrum of PS for low and high values of the MCP voltage, V_C, are shown in Fig. 2. At a V_C value of 650 V, the high mass cationised PS oligomer distribution is only weak. The full distribution is revealed at the higher voltage. The effect of V_C on the detection efficiency for ions of different mass is shown in Fig 3. Efficiencies rise steeply before reaching a plateau, as expected. The voltage necessary to reach the plateau increases with mass. It is evident that relative ion intensities along the mass scale will vary sensitively with the value of V_C. A method is therefore required to allow users to set the detector voltage to give a known efficiency and reduce spectrum variability. A very simple procedure, developed by Seah [31] for CEMs, may be applied here. The transition voltage, V_T, which provides 50% of the plateau efficiency, may be quickly and accurately determined because of the steep efficiency gradient. The effect of ion mass on V_T for cationised polystyrene oligomers is shown in Fig. 4. The higher voltage,

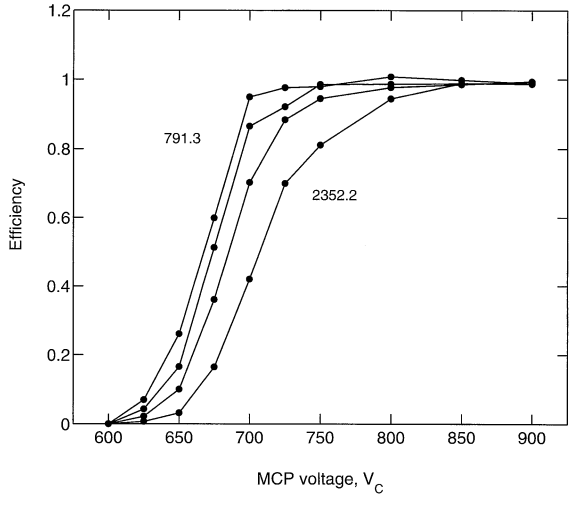

Fig. 3. Effect of MCP voltage on the detection efficiency of cationised PS oligomers with masses 791.3, 1103.5, 1519.8 and 2352.2.

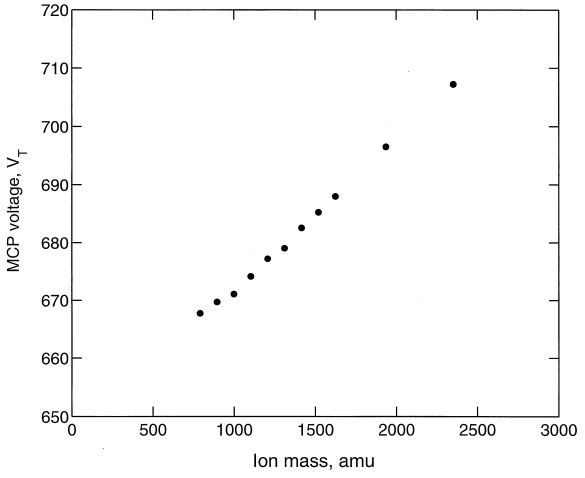

Fig. 4. MCP transition voltage, V_T, required to give 50% of the plateau detection efficiency.

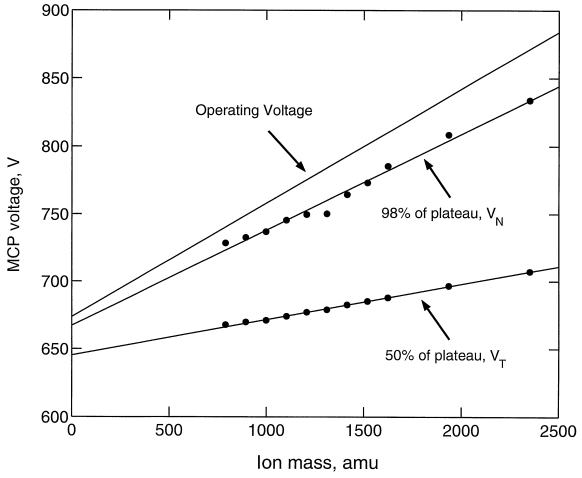

Fig. 5. MCP operating voltage together with V_T and V_N.

V_N, required to increase the detection efficiency to 98% together with the values of V_T are shown in Fig 5. Straight-line fits to these data give the necessary increase in voltage. The operating voltage, V, is now defined as a factor of 1.3 more than $(V_N - V_T)$, for safety, in addition to V_T, such that

$$V = V_T + 29.1 + 0.0572\ m \quad (3)$$

where m is the ion mass and V is in volts. To prevent damage and reduce aging, the detector should not be operated at too high a voltage, so Eq. (3) is limited to a maximum of 950 V. To ensure that the efficiency is at least 98%, the detector voltage should be set for the highest mass ion in the required mass range. As the MCP ages, the value of V_T for a given mass will increase; therefore, the operating voltage should be calibrated at regular intervals and monitored using a control chart. The use of V_T allows one to do this with great precision so that the need to replace the MCP can be predicted in advance. For the remainder of this study the detector voltage was set at 875 V, which gives approximately unity detection efficiency for all measured masses at ion impact energies of 20 keV.

3.2. Effect of ion mass, energy and composition

The positive ion static SIMS spectra from PS samples are shown in Fig. 6(a,b) for post-acceleration voltages of 2 kV and 20 kV. While the low-mass regions of 0–300 amu are similar, the intensities of the cationised PS oligomers are reduced by nearly two orders of magnitude for the lower energy. The effect of ion impact energy on the detection efficiencies for oligomers ranging in mass from 791.3 to 2352.2, are shown in Fig. 7(a). The data are replotted in Fig 7(b) for the ion impact velocity. With this detector system it is not possible to measure the secondary ion current with a picoammeter for each mass to calculate an absolute efficiency. The currents are simply too small. Instead, the data have been normalised to unity efficiency at 20 keV. At energies greater than 15 keV, the peak intensities are relatively constant with impact

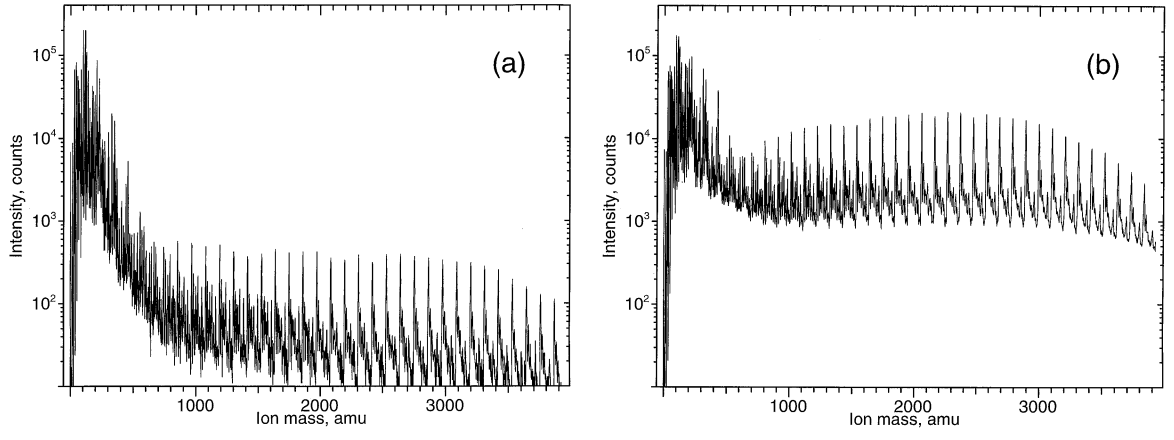

Fig. 6. Positive ion SIMS spectra of Ag cationised PS (MW 2,500) with post-acceleration voltages of (a) 2 kV and (b) 20 kV.

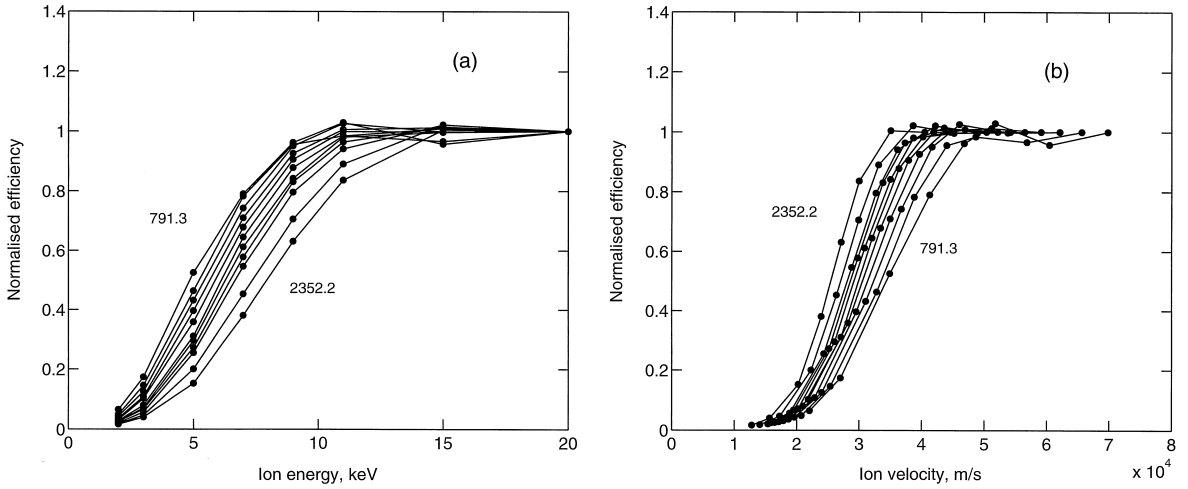

Fig. 7. Normalised secondary ion intensities for cationised PS oligomers, with repeat units from 6 to 21 corresponding to masses between 791.3 and 2352.2, plotted against (a) ion impact energy and (b) ion impact velocity. The masses for the outer curves are shown.

energy. The families of curves in Fig 7 show how rapidly the detector efficiency falls as the ion impact energy is reduced or the mass is increased. Additionally, for a given ion impact velocity, the efficiency and consequently the yield is greater for the larger molecules than for the smaller ones.

Using a post-acceleration voltage, V_D, of 20 kV it is only possible to extend the normalisation method, mentioned above, so far up the mass scale. Eventually, at a high enough mass, there will be no plateau in the energy range available. To analyse this effect, we fit a model to the data using a function to describe the ion-induced secondary electron yield and our knowledge of the behaviour of a continuous dynode detector.

Whereas the models, discussed earlier, for kinetic electron emission have provided much insight into the mechanisms of emission, they have limited applicability at the low velocities used in this study. Instead, we use a simple function in terms of velocity, v, with three independent variables, a scaling item A, the usual "straight-line threshold" velocity v_0 and a power n, such that

$$\gamma = Av\left(1 - \left(\frac{1}{1 + (v/v_0)^n}\right)^{1/n}\right) \quad (4)$$

At high velocities, this function reduces to the linear function of velocity as predicted by the theory of Sternglass. This function gives excellent fit to the data of Brunelle et al. [15] for large organic molecules of bovine trypsin (MW 23, 295 amu) on a CsI surface with values for n and v_0 of 3.4 and 1.98×10^5 m/s respectively and also to the data of Hofer [32] for vanadium clusters incident on gold with values for n and v_0 of 4.7 and 1.71×10^5 m/s, respectively. It also describes the general behaviour of the Parilis and Kishinevski model [23] and does not have the arbitrary change in behaviour between each of the three regions of velocity dependence that is often used in approximations to this model.

The theory for the efficiency of CEM detectors for electrons is already well established [2–6]. The emission of secondary electrons at each stage in the dynode has a Poisson probability distribution. Therefore, at each stage in the amplification there is a finite possibility that the cascade will die. The detector efficiency is then calculated by summing the losses at each stage using Eq. (6) of Ref. 2. This may be evaluated provided that the values for the secondary electron yield are known at each stage. In our system, the first emission stage is induced by ions and γ is given by Eq. (4). The value of γ for subsequent stages depends on the potential difference along the dynode. Seah [2] found a value of 2 was acceptable and this value is used here.

In our model, we will assume that the yield for a

Table 1
Values of v_0 found from a survey of the literature

Impact ion	Target	v_0 10^4 m/s	Reference
Ar	Mo	10.7	24
Ne	Cu-Be	6.15	33
Ar		5.38	
C_7H_{16}	Cu	4.0	25
D	Ag	25.0	34
V	Stainless steel	4.38	35
Nb		3.44	
$(H_2O)_n$ [n = 320 to 3311]	Cu	4.14	27
$(H_2O)_n$ [n = 320]	Cu	4.59	28
Xe	Au	8.49	36
$C_{16}F_{31}$	—	2.75	12

polyatomic ion is simply the sum of the constituent yields, i.e., additivity is obeyed. For our series of cationised PS oligomers, where the composition of H and C is approximately constant, the yield is proportional to the number of repeat units and consequently the mass. The effect of the silver cation is always less than 1% of the composition and so is ignored here. We therefore replace the general scaling term A with a coefficient a multiplied with the ion mass. To evaluate the detector efficiency, the three independent variables a, v_0 and n of Eq. (4) are required. These are found in the following way. Firstly, an approximate value for v_0 may be obtained from a survey of the literature. Table 1 gives the values of v_0 for a range of ion target combinations, including polyatomic ions, from data over the last four decades. Notwithstanding the variety of experiments, the values are reasonably consistent with an average value, excluding the deuterium data, of 5.4×10^4 m/s. With this value as a first estimate of v_0 the variables a and n are fitted using a computer algorithm to the efficiency curves of Fig. 7 for each ion. The algorithm starts with trial values of 1×10^{-4} and 3.5, respectively, for the two parameters and calculates γ for each ion energy. This value is then input to the model by Seah [2] as the first emission event, which then gives an efficiency at each energy. The fitting minimisation proceeds using the least squares of the residuals. Excellent fits are found, but the values of the variables are rather scattered as they are correlated. As the mass of each oligomer is increased we are simply adding another unit of C_8H_8, and so the coefficient a would, therefore, be expected to remain constant. Values of a equal to 2×10^{-6} m/s and n equal to 4.9 are then taken as the average of the fitted values. Finally, the fitting is made with only one scaling parameter v_0. The fits and data for four of the ions are shown in Fig. 8. The fitted results using Eq. (4) are clearly excellent. Figure 9 shows values of v_0, which exhibit clear systematics with ion mass. The solid line in Fig. 9 is a power law function fit with an index of -0.13.

The systematic power law dependence of v_0 enables the detector efficiency for PS oligomers to be calculated for any mass and for any post-acceleration voltage. Fig. 10 shows a family of such curves together with the data points and Fig 11 the deduced values of γ for two ions. The curves of efficiency fit the data excellently. Most modern TOF SSIMS spectrometers have a post-acceleration voltage of 10 kV. For this condition, beyond a mass of 1000 amu, the detector efficiency rolls off, falling to 80% at 2000 amu, 50% efficiency at 4000 amu and at 10,000 amu to 20%. In contrast, with a post-acceleration voltage of 20 kV the efficiency remains at unity to 4000 amu, slowly declining to 80% efficiency at 10,000 amu. By using a post-acceleration voltage of 20 kV, the relative spectral intensities are less sensitive to the precise instrument conditions used and have near unity detection efficiency. Many older TOF spectrometers have a post-acceleration voltage of only 5 kV. In that case, the efficiency is already as low as 20% at 2000 amu. Quadrupole mass analysers using CEMs often use voltages as low as 3 kV. In that case, detector efficiencies fall rapidly with mass for masses above 100 amu. In comparisons of the transmission between quadrupole and time-of-flight mass analysers, this effect is generally not included and will add to the inherent differences of the mass spectrometers.

What we see in Fig. 10 is the effect of g_1 in Eq. (2). As the fragment mass (number of constituent atoms) increases, the total secondary electron yield falls and the proportion of failed cascades increases. Thus, the efficiency falls. The reduction in yield has a secondary effect in that the successful cascades have a proportion with a slightly smaller pulse height distri-

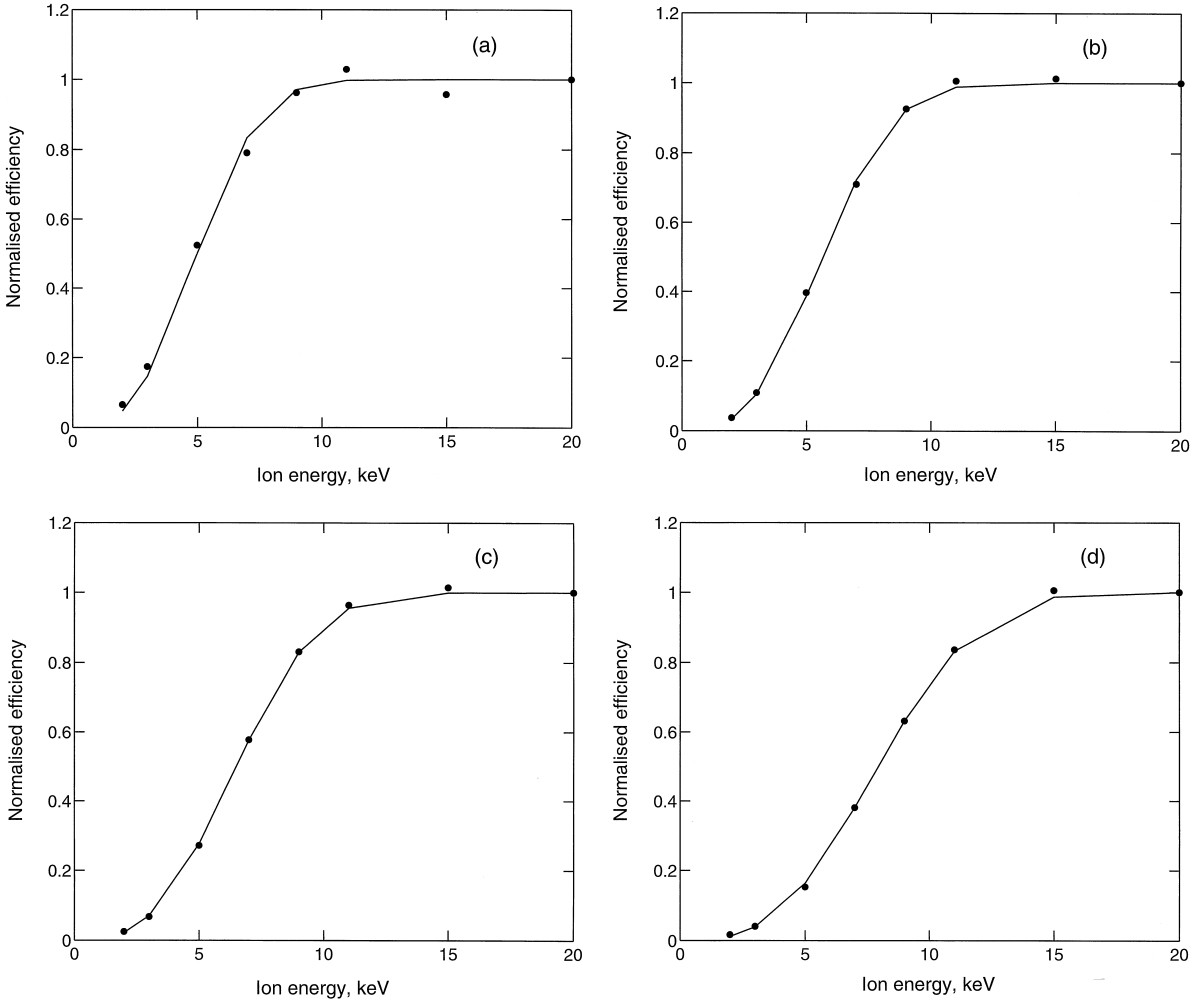

Fig. 8. Fits to detection efficiency against ion energy (solid line) together with data values (●) for ion masses (a) 791.3, (b) 1103.5, (c) 1519.8 and (d) 2352.2.

bution. This pulse height distribution thus also falls as the fragment mass (number of constituent atoms) increases, which needs to be countered by an increase in the MCP voltage, V_C, as shown in Fig. 5. If V_C is below the value set by Eq. (3), the fall in efficiency in plots like Fig. 10 becomes even more severe as the mass increases.

The efficiency curves are similar to those calculated by Niehuis [12] using Cr clusters, which show a drop to an efficiency of 42% at mass 7488. This is somewhat lower than calculated here. A cluster at this mass has 144 Cr atoms and the equivalent PS oligomer would have one Ag, 568 C and 563 H atoms. In both cases, the impact velocity is the same for each component atom. Hydrogen has a rather small total stopping power and so its contribution to the overall electron emission will be small.

It is clear that the overall emission will depend on the composition of the ion. If the emission yield for C is greater than 144/568 that of Cr, the detection efficiency would be higher. The curves shown in Fig. 10 for PS would, in the more general case for any fragments, be bands that depend on the fragment composition. We study this behaviour below. The

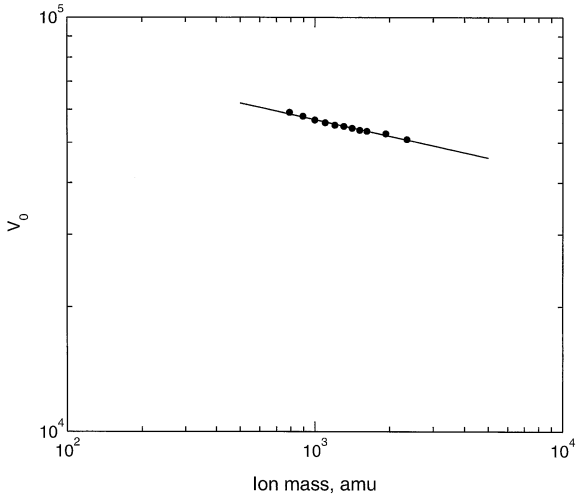

Fig. 9. Values of the fitted velocity threshold v_0 against mass. The solid line is a power law fit to the data points.

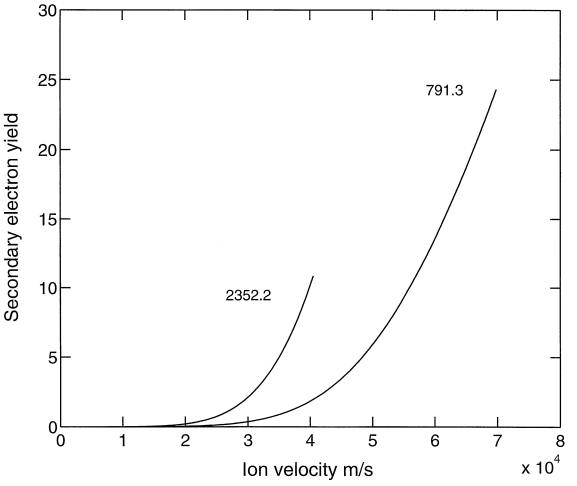

Fig. 11. Secondary electron yield, γ, deduced from the fits of detection efficiency in Figs 8(a) and (d).

extent of these bands can be estimated by calculating the contribution to the total yield from each atomic species. Here we use Beuhler and Friedman's [25] model, based on the total stopping power, to calculate the electron emission yield for different atomic number ions relative to carbon. A cluster with a mass of 4000 amu and an energy of 10 keV impacts the detector at a velocity of 2.2×10^4 m/s. Each constituent atom has the same velocity. The electron yields are evaluated for elemental ions at this velocity

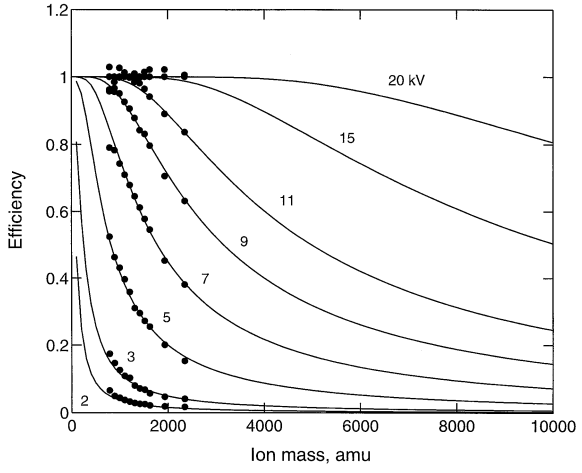

Fig. 10. Calculated PS oligomer detection efficiency curves, for the different ion impact energies shown, together with measured values (●).

impacting a target with an average atomic number of 20 and a secondary electron transport length of 1.04 nm [25]. The calculated secondary electron yields relative to C for H, N, O, Cr and Ag ions are 0.017, 1.321, 1.670, 11.123 and 29.952, respectively. Secondary electron yields may now be estimated, by summation of the component yields, for ions from four archetypal materials of different compositions; a chromium cluster, cationised polystyrene oligomers, a biological material based on adenine and thymine, and a saturated hydrocarbon. These ions have the following compositions of Cr_{77}, $AgC_{300}H_{295}$, $C_{153}H_{168}O_{31}N_{107}$ and $C_{286}H_{572}$, respectively. Electron yields relative to the PS oligomers are then 2.56, 1, 1.04 and 0.88 for the chromium cluster, PS oligomer, biomaterial and hydrocarbon. These factors may be used to scale the term *A* in Eq. (4), assuming that the relative scalings are approximately independent of velocity. Fig. 12(a) shows a band covering the curves of Fig 10 recalculated for these different ion compositions. Each shaded area covers all four materials but is always limited by chromium cluster ions at the top of the band and saturated hydrocarbons at the bottom.

For analysts working with a wide range of compositions, the variation in detector efficiency with composition is surprisingly large. Using a post-accelera-

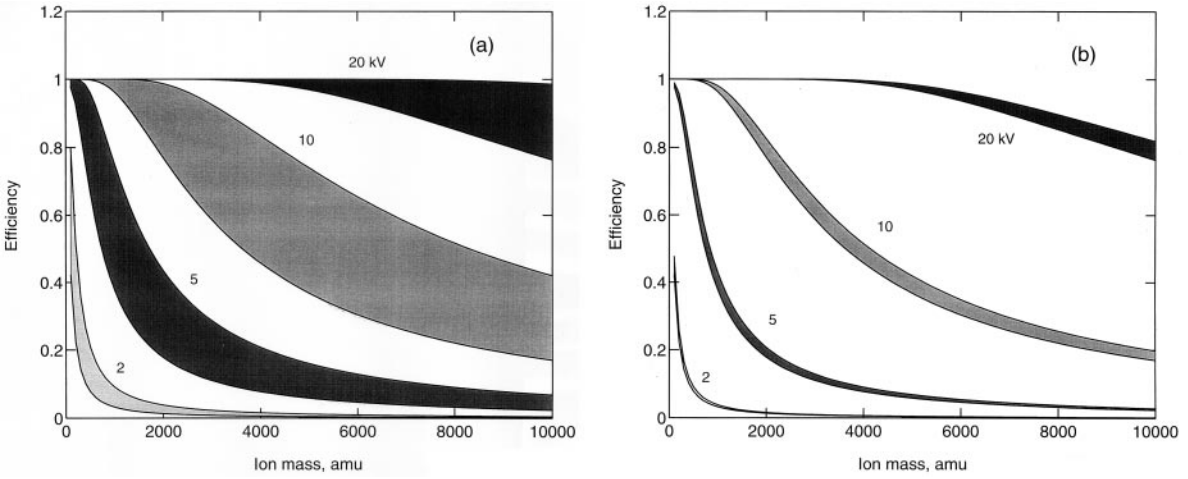

Fig. 12. Estimated detection efficiency ranges of different ion compositions for post-acceleration voltages, V_D, of 2, 5, 10 and 20 kV for (a) chromium cluster ions and organics and (b) organics only.

tion voltage of 20 kV or above reduces this significantly, so that for ions below 4000 amu the efficiency is effectively unity. Fig. 12(b) shows the case for an analyst whose work is generally restricted to organic ions. The limit at the top of each shaded area is now that deduced for the biomaterial and at the bottom, again, for hydrocarbons. The variation with composition is now much smaller. These lower detection efficiencies arise from the higher hydrogen contents of the ions. To improve the detector efficiency for heavy ions and to reduce the variability from differing compositions, it is recommended that analysts use the highest value of post-acceleration voltage available to them.

We now return to the data and predictions for polystyrene. It is useful to know, for a given mass, what value of post-acceleration voltage is necessary to achieve a specified detector efficiency. Fig. 13 shows such curves calculated from our model for PS oligomers. To work with a detection efficiency of 99% for ions of up to 10,000 amu requires a post-acceleration voltage of 35 kV. Such high voltages are not normally available in SIMS instrumentation. Many are limited to 10 kV, and for these an efficiency of 99% is only achievable up to 850 amu.

The effect of detector aging is an added effect of practical importance and may also be calculated using this model. Figure 14 shows, for the PS oligomer data of Fig. 10, what happens as the detector ages and the secondary electron yield of the first event falls to half its original value. The original data are shown by a solid line and the aged data by the dashed line. This will lead to a relative loss of high mass intensity compared with low masses. The variations are more pronounced for lower values of post-acceleration voltage. For all purposes it is clear that high values of post-acceleration voltage are best.

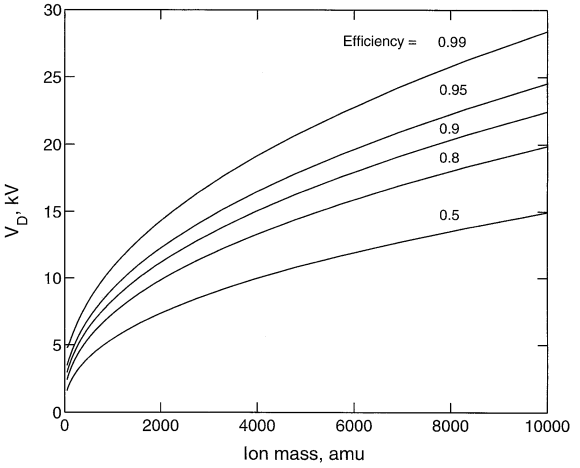

Fig. 13. Value of post-acceleration voltage, V_D, required to attain detector efficiencies of 0.5, 0.8, 0.9, 0.95 and 0.99.

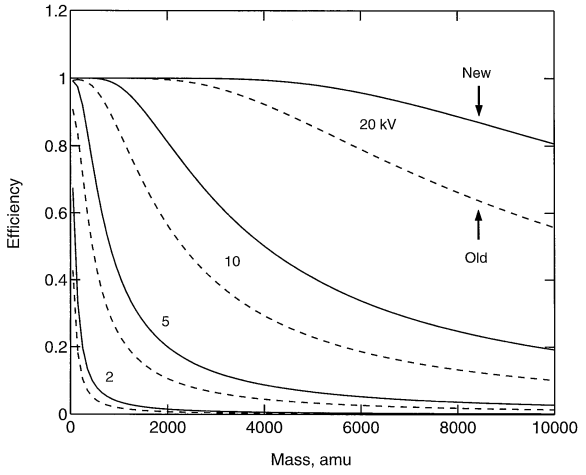

Fig. 14. Detection efficiencies calculated for a new (——) and aged (- - -) detector for post-acceleration voltages, V_D, of 2, 5, 10 and 20 kV.

4. Conclusions

The detection efficiency of a microchannel plate (MCP) for high mass cationised PS oligomer ions has been measured. The effect of the ion impact energy, between 0 and 20 keV, at the front of the MCP is studied, and a model is developed based on a function to describe the ion-induced electron emission and a general theory for CEMs [2]. For polyatomic ions, this function uses the additive nature of electron yields from the individual component atoms. Values of the straight-line threshold velocity, v_0, are found to have a weak power law dependence on mass with an index of -0.13.

The model is an excellent description of the data and shows how the efficiency falls away as the mass increases or the ion impact energy reduces. At a mass of 10,000 amu, the detection efficiency for 20 keV ions is 80%, falling to 25% for 10 keV ions. In a TOF spectrometer the ion impact energy is controlled by the post-acceleration voltage. If this is set to 20 kV, approximately unity detection efficiency may be achieved for masses up to 4000 amu.

Estimates of the variation in detection efficiency with ion composition have been calculated for compositions ranging from hydrocarbons through biomaterials to elemental clusters. It is found that the effect of composition is strong. For low-energy ion impacts, the spread in efficiency may be more than 100% of the mean efficiency. This effect reduces as the ion impact energy is increased. At an energy of 20 keV, the detection efficiency remains near unity for all clusters with masses of up to 4000 amu.

A method of setting the detector voltage regularly, using an accurate and simple procedure is given. Here, the voltage at half the plateau intensity, V_T, may be quickly determined for the highest mass ion to be analysed. The detector voltage should then be set to a voltage in excess of V_T, given by Eq. (3), to give the best efficiency.

Acknowledgements

The authors would like to thank S. Kayser of ION-TOF for details of the MCP used in this study and Dr. E. Niehuis for a copy of his thesis. This work forms part of the Valid Analytical Measurement programme supported by the National Measurement System Policy Unit of the Department of Trade and Industry.

References

[1] J. Ladislas Wiza, Nucl. Instr. Methods B 162 (1979) 587.
[2] M.P. Seah, J. Electron Spectrosc. 50 (1990) 137.
[3] M.P. Seah, C.S. Lim, K.L. Tong, J. Electron Spectrosc. 48 (1989) 209.
[4] M.P. Seah, G.C. Smith, Rev. Sci. Instrum. 62 (1991) 62.
[5] M.P. Seah, M. Tosa, Surf. Interface Anal. 18 (1996) 240.
[6] M.P. Seah, Surf. Interface Anal. 23 (1995) 729.
[7] I.S. Gilmore, M.P. Seah, NPL Report CMMT(A)87 (1998).
[8] I.S. Gilmore, M.P. Seah, Appl. Surf. Sci. 144-145 (1999) 113.
[9] I.S. Gilmore, M.P. Seah, in G. Gillen, R. Lareau, J. Bennet, F. Stevie (Eds.), SIMS, vol. XI, John Wiley, Chichester, 1998, p. 999.
[10] M.A. Rudat and G.H. Morrison, Int. J. Mass Spectrom. Ion Processes 27 (1978) 249.
[11] R. Hinton, private communication (1997).
[12] E. Niehuis, Doctoral thesis, Münster (1988).
[13] B. Hagenhoff, A. Benninghoven, H. Barthel, W Zoller, Anal. Chem. 63 (1991) 2466.
[14] A. Brunelle, P. Chaurand, S. Della-Negra, Y. Le Beyec, G.B. Baptisce, Int. J. Mass Spectrom. Ion Processes 126 (1993) 65.

[15] A. Brunelle, P. Chaurand, S. Della-Negra, Y. Le Beyec, E. Parlis, Rapid Commun. Mass Spec. 11 (1997) 353.
[16] V. Tan Nguyen, K. Wien, Nucl. Instr. Methods B, 145 (1998) 332.
[17] J. Mootens, W. Ens, K.G. Standing, A. Verentchikov, Mass Spec. 6 (1992) 147.
[18] G. Westmacott, W. Ens, K.G. Standing, Nucl. Instr. Methods B, 108 (1996) 282.
[19] A. Hedin, P. Håkansson, B.U.R. Sundquist, Int. J. Mass Spectrom. Ion Processes 75 (1987) 275.
[20] Y. Le Beyec, Int. J. Mass Spectrom. Ion Processes 174 (1998) 107.
[21] K.H. Krebs, Fortschritte der Physik 16 (1968) 419.
[22] R.A. Baragiola, E.V. Alonso, J. Ferron, A. Oliva-Florio, Surf. Sci. 90 (1979) 240.
[23] E.S. Parilis, L.M. Kishinevski, Soviet Phys.-Solid State 3 (1960) 885.
[24] U.A. Arifov, R.R. Rakhimov, Isv. Akad. Nauk SSSR, Ser. Fiz. Mat. 6 (1958) 49.
[25] R.J. Beuhler, L. Friedman, J. Appl. Phys. 48 (1977) 3928.
[26] E.J. Sternglass, Phys. Rev. 108 (1957) 1.
[27] R.J. Beuhler, L. Friedman, Nucl. Instr. Methods B 170 (1980) 309.
[28] R.J. Beuhler, J. Appl. Phys. 54 (1983) 4118.
[29] J. Schwieters, H-G. Cramer, T. Heller, U. Jürgens, E. Niehuis, J. Zehnpfenning, A. Benninghoven, J. Vac. Sci. Technol. A9 (1991) 2864.
[30] I.S. Gilmore, M.P. Seah, unpublished.
[31] M.P. Seah, VAM Bull. 10 (1993) 23.
[32] W.O. Hofer, Scanning Microsc. Suppl. 4 (1990) 265.
[33] B.L. Schram, A.J.H. Boerboom, W. Kleine, J. Kistemaker, Physica 32 (1966) 749.
[34] R.A. Baragiola, E.V. Alonso, A. Oliva Florio, Phys. Rev. B 19 (1979) 121.
[35] F. Thum, W.O. Hofer, Surf. Sci. 90 (1979) 331.
[36] E.V. Alonso, M. Alurralde, R.A. Baragiola, Surf. Sci. 166 (1986) L155.